Sensors and Materials, Vol. 35, No. 5 (2023) 1569–1577
MYU Tokyo

S & M 3270

Inhibition of Brookite Phase of TiO_2 via Addition of Dimethylformamide Solvent and Annealing

Pao-Hsun Huang,[1] Yu-Quan Zhu,[1] Li-Wei Chao,[2] Wei-Chin Lin,[2] Rui-Xian Zheng,[2] Kuan-Wei Lee,[2*] and Chien-Jung Huang[3**]

[1]School of Ocean Information Engineering, Jimei University, Jimei District, Xiamen 361021, Fujian, China
[2]Department of Electronic Engineering, I-Shou University, Kaohsiung 84008, Taiwan
[3]Department of Applied Physics, Nation University of Kaohsiung, Kaohsiung University Road, Kaohsiung 81148, Taiwan

(Received August 1, 2022; accepted December 1, 2022)

Keywords: titanium dioxide, DMF, brookite, annealing

Annealing can usually inhibit the formation of an unstable brookite mesophase in the crystal structure, enhancing the growth of an anatase titanium dioxide (TiO_2) thin film. In this study, after a TiO_2 solution was prepared with and without a small amount (1 wt%) of the organic solvent dimethylformamide (DMF), TiO_2 films were obtained by dynamic spin-coating and were annealed at temperatures of 300, 500, and 700 °C. The structural and optical properties as well as the surface morphologies of the films were studied. The experimental results show that the TiO_2 film annealed at 500 °C exhibits a polycrystalline anatase and brookite multiphase and usefully inhibits the formation of the brookite mesophase when annealed at 700 °C. Moreover, adding the DMF effectively contributes to the formation of the polycrystalline phase at 300 °C. The compactness of the annealed TiO_2 film was improved by adding 1 wt% DMF, as shown by topographic images obtained by atomic force microscopy, leading to decreased transmittance and increased absorbance. The band gap (*Eg*) values of all the samples were also estimated. The variation of *Eg* was evidenced by the structural change and the redshift of the absorption edge.

1. Introduction

In the last decade, the abundant metal oxide TiO_2 has been applied to many emerging optoelectronic devices, such as gas sensors,[1] solar cells,[2] LEDs,[3] photocatalysts, and gate insulators in metal-oxide-semiconductor field-effect transistors.[4–6] The properties of TiO_2, including its structural, optical, electrical, and chemical properties,[7,8] and its synthesis technique[9] have been extensively studied by many research groups.[10–12] Among the various technologies developed for preparing TiO_2 films, such as chemical vapor deposition, E-beam processing, thermal evaporation, and atomic layer deposition,[13–16] solution preparation is the most convenient and low-cost method[17] and has been widely used because the required equipment can be easily assembled. The TiO_2 film quality depends on not only the arrangement

*Corresponding author: e-mail: kwlee@isu.edu.tw
**Corresponding author: e-mail: chien@nuk.edu.tw
https://doi.org/10.18494/SAM4062

ISSN 0914-4935
https://myukk.org/

of the Ti and oxygen atoms during the deposition process but also the post-treatment, such as classical annealing and solvent presynthesis.

Annealing is usually applied to improve the compactness and crystal structure of films, both of which are strongly influenced by the annealing temperature. Studies related to the annealing of TiO_2 have mainly focused on preparation by the sol-gel method, a solution method, or physical sputtering.[18,19] The crystal structure of TiO_2 has been reported to have three phases: the anatase phase and rutile phase, which respectively exist below 600 °C and above 800 °C, and the brookite mesophase, which is the transition phase before the crystallization of the anatase phase. Because of the interaction of the thermodynamic variables, notably the surface energy, the crystal phase of TiO_2 also depends on the particle size.[20] Nanocrystalline particles can develop in sol-gel films, despite this normally being a problem with nanoparticles. Adding a solvent is a useful way of forming the anatase phase. However, few studies have reported the effects of an organic solvent on the brookite mesophase of a TiO_2 film. The organic solvent dimethylformamide (DMF) is promising for improving the properties of TiO_2 films, mainly due to its reactivity and its ability to increase the compactness of films.[9,21] The variation of the crystal structure with the amount of added DMF is worth researching, as well as the influence of the annealing temperature. The resulting difference in optical properties may be attributed to the formation of the brookite mesophase. This mesophase is not stable during the deposition and has no industrial application.

In this study, TiO_2 films are prepared with and without 1 wt% DMF solvent in the solution. The films are annealed at 300, 500, and 700 °C, and the effects of the addition of DMF and the annealing temperature on the structural and optical properties of the films and their surface morphologies are investigated. The optical band gap (*Eg*) of the films is also estimated. Finally, we discuss whether the brookite mesophase of the films is inhibited by the DMF solvent and by increasing the annealing temperature.

2. Materials and Methods

2.1 Preparation and methods

The materials were purchased from commercial sources and used without further purification. The preparation parameters for the TiO_2 precursor solution and the static spin-coating method are shown in Table 1. There are two reasons for choosing DMF as the organic solvent. Firstly, its high boiling point of around 150 °C, resulting in a low evaporation rate, increases the stability and reproducibility of the synthesis conditions. Secondly, DMF is widely used for the reduction of metal ions and to slow the hydrolysis of titanium alkoxides. As shown in Fig. 1, to prepare the TiO_2 precursor solution, titanium isopropoxide [$Ti(OCH(CH_3)_2)_4$] and HCl solution were diluted in isopropanol (C_3H_8O). Then, these two diluted solutions were mixed [with the diluted HCl solution added dropwise to the diluted $Ti(OCH(CH_3)_2)_4$ solution], and the mixture was continuously stirred at 300 rpm for 24 h. The TiO_2 precursor was then filtered with a polytetrafluoroethylene (PTFE) filter with a 0.2 μm pore size before use.

Table 1
Preparation parameters for the TiO_2 precursor solution, the static spin-coating method, and the annealing.

Parameter	Value	Unit	Note
Titanium isopropoxide, $Ti(OCH(CH_3)_2)_4$	369	µl	Sigma-Aldrich
Isopropanol, C_3H_8O	2.53	ml	
HCl (concentration of 2 M)	35	µl	
Dimethylformamide, DMF	1	wt%	
Rotation speed	1000 / 3000	rpm	two-step
Rotation time	10 / 60	s	two-step
Heating temperature	180	°C	
Heating time	5	min	
Annealing temperature	300/500/700	°C	
Annealing time	30	min	
Heating rate	5	°C · min^{-1}	
Annealing gas	Atmosphere		

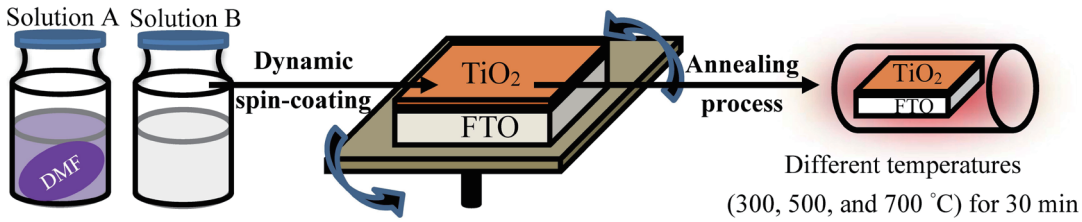

Fig. 1. (Color online) Schematic of deposition process.

We cleaned 2 × 2 cm^2 fluorine-doped tin oxide (FTO) glass substrates of 7 Ω/sq sheet resistance (AimCore Technology, Hsinchu, Taiwan) with a detergent solution, deionized (DI) water (DI-water), acetone, methanol, and DI water for 5 min each, then dried them at 105 °C for 30 min after blowing nitrogen gas. The FTO substrates were further treated with oxygen (O_2) plasma at 10 W for 2 min (Junsun Tech. Co., Ltd., Taipei, Taiwan). Next, a TiO_2 layer was deposited on the substrates via the static spin-coating method in a glove box. The moisture and O_2 concentrations in the glove box were maintained at lower than 10 ppm. The samples were heated at 180 °C for 5 min on a hotplate in the glove box then annealed at a temperature of 300, 500, or 700 °C for 30 min.

2.2 Measuring equipment

The TiO_2 thin films were measured by X-ray diffraction (XRD, Ultima IV, Rigaku Corporation, Tokyo, Japan) to determine their crystallite structure. The top-view surface and 3D morphologies were measured over a 5 × 5 μm^2 area by atomic force microscopy (AFM, XE-70, Park Systems, Suwon, Korea) with a scan rate of 0.5 Hz. The optical properties of the samples, including the transmittance, reflectance, and absorption, were detected, and a spectrophotometer (UV-3900, Hitachi, Tokyo, Japan) was used to estimate *Eg*.

3. Results and Discussion

A schematic diagram of the annealing process for temperatures of 300, 500, and 700 °C is shown in Fig. 2. The horizontal solid lines with arrows and the dotted lines represent the annealing time at the set temperature (30 min) and the cooling time to room temperature, respectively.

To determine the crystalline structure, we obtained the XRD patterns of the TiO_2 films prepared with and without 1% DMF solvent then annealed at 300, 500, and 700 °C, which are shown in Fig. 3. The peaks at 2θ = 25.47, 32.86, 37.34, 47.2, 51.93, 54.76, and 62.15° correspond to phases of the anatase (A) and brookie (B) families of A(101), B(020), A(004), A(200), A(105), A(211), and A(204), respectively (JCPDS card nos. 83-2243 and 75-1582). No peaks were observed for the sample prepared without DMF solvent followed by annealing at 300 °C. This is in good agreement with the results of other research involving thermal engineering, demonstrating that deposition below 300 °C generates amorphous TiO_2 films.[22] At 500 °C, the film structure changes from an amorphous phase to a polycrystalline phase (anatase and brookie structures) owing to the reorganization of Ti and O atoms. The reorganization results from the

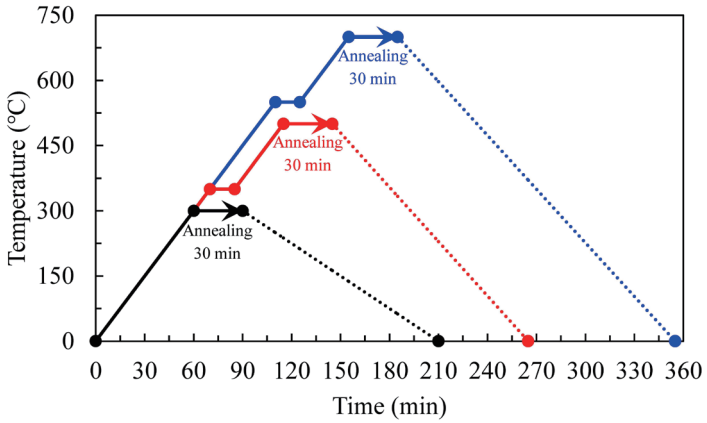

Fig. 2. (Color online) Schematic diagram of annealing timeline at temperatures of 300, 500, and 700 °C.

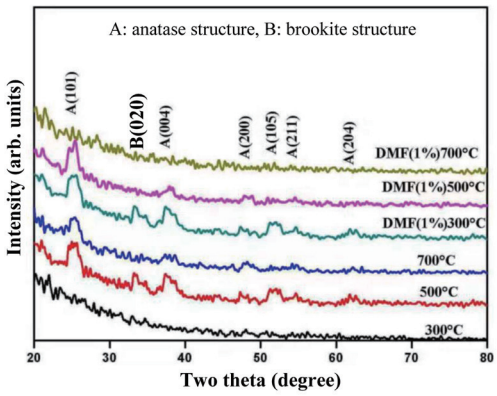

Fig. 3. (Color online) XRD patterns of TiO_2 thin films with and without 1.0% DMF solvent after annealing at temperatures from 300 to 700 °C.

annealing, which causes the movement of atoms and lattice vacancies in the film to release the internal microstrain and also eliminate the differential arrangement. When the annealing temperature is increased to 700 °C, however, the B(020) and A(105) peaks observed at 33.34° and 51.93° disappear. The TiO_2 film prepared with DMF (DMF-TiO_2 film) also shows a polycrystalline phase at 300 °C, demonstrating that the crystalline structure and the compactness of the film can be improved by using volatile DMF. This result has been reported elsewhere.[23,24] When the annealing temperature is increased to 500 and 700 °C, the B(020) peak at 33.34° is inhibited and the film structure also changes from polycrystalline at 500 °C to amorphous at 700 °C. The annealing at 500 °C clearly inhibits the growth of the B(103), A(105), and A(204) peaks. The insufficient amount of DMF added may have been the reason for the gradual phase transition from 500 to 700 °C. Moreover, a decrease in the annealing temperature required for crystallization upon adding DMF is evidenced, and a trace amount of DMF can also assist the growth of the B(103) peak at 300 °C.

The surface roughness of the DFM-TiO_2 films is also improved, according to the AFM measurement. The topographic and surface morphologies of DMF-TiO_2 films annealed from 300 to 700 °C are determined by AFM, as shown in Figs. 4(a)–4(c), respectively. The root-mean-square surface roughness (Rq) values evaluated at 300 and 500 °C are respectively ~2.3 and ~2.28 nm. Then, Rq slightly increases to its highest value of 2.62 nm at 700 °C, revealing that adding DMF effectively keeps the surface at a similar level of roughness.

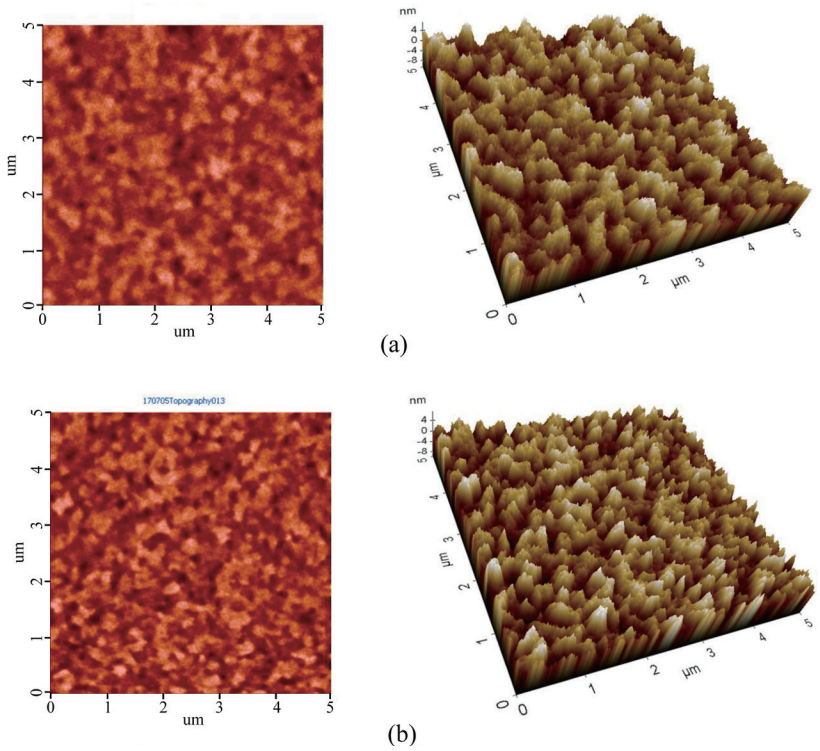

Fig. 4. (Color online) Topographic and surface morphologies of DMF-TiO_2 films after annealing at temperatures of (a) 300 °C, (b) 500 °C, and (c) 700 °C.

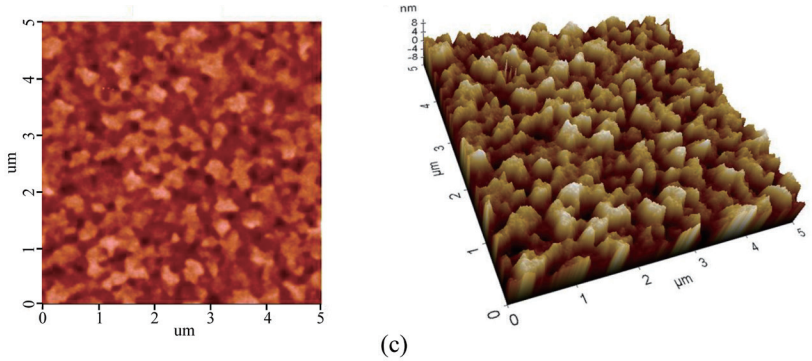

Fig. 4. (Continued) (Color online) Topographic and surface morphologies of DMF-TiO_2 films after annealing at temperatures of (a) 300 °C, (b) 500 °C, and (c) 700 °C.

Figure 5 shows the optical properties, including the transmittance, reflectance, and absorption spectra, for the annealed TiO_2 and DMF-TiO_2 films at different temperatures as a function of wavelength from 350 to 850 nm. At the annealing temperature of 300 °C, the transmittance of DMF-TiO_2 is slightly higher than that of the TiO_2 film, possibly owing to the crystallization resulting from the addtion of DMF [Fig. 5(a)]. The small amount (1 wt%) of solvent induces crystal rearrangement, resulting in a slight increase in the transmittance of the film. Moreover, this increase in transmittance is mainly observed at short wavelengths (350–450 nm). Similar behavior was observed with annealing temperatures of 500 and 700 °C. However, the DMF-TiO_2 film annealed at 700 °C has a lower transmittance (~4%) than that of the TiO_2 film at long wavelengths (650–850 nm). This is mainly attributed to the increasing film compactness resulting from the addition of DMF solvent, as reported in many studies.[9,21] With increasing annealing temperature from 300 to 500 °C, the reflectance of the TiO_2 films slightly decreases at long wavelengths (550–850 nm) but slightly increases at short wavelengths (350–600 nm) when the annealing temperature is increased to 700 °C. However, with increasing annealing temperature from 300 to 500 °C, the DMF-TiO_2 films show decreased reflectance at short wavelengths (350–550 nm) but increased reflectance when the annealing temperature is increased to 700 °C. These properties can be attributed to enhanced absorption in the UV range caused by the greater compactness induced by adding DMF solvent. Another reason may be the optical loss caused by haze.[25] Therefore, as shown in Fig. 5(b), the absorbance of the samples increases with increasing annealing temperature, which is the opposite trend to the transmittance. This result suggests that the increased compactness of the film contributes to the increased absorbance, as similarly observed elsewhere.[7] We estimate the influence of the sample thickness and reflection by calculating the absorption coefficient (α) of the films using the Beer–Lambert law:

$$\alpha(\lambda) = (-1/d)\ln[T(\lambda)/(1-R^2(\lambda))], \quad (1)$$

where α is the absorption coefficient, λ is the wavelength inside the medium with largest d, and T and R are the transmittance and reflectance, respectively. The band gap Eg of the films was obtained from a Tauc plot [Fig. 5(b)], which is a plot of α versus the wavelength, using[26]

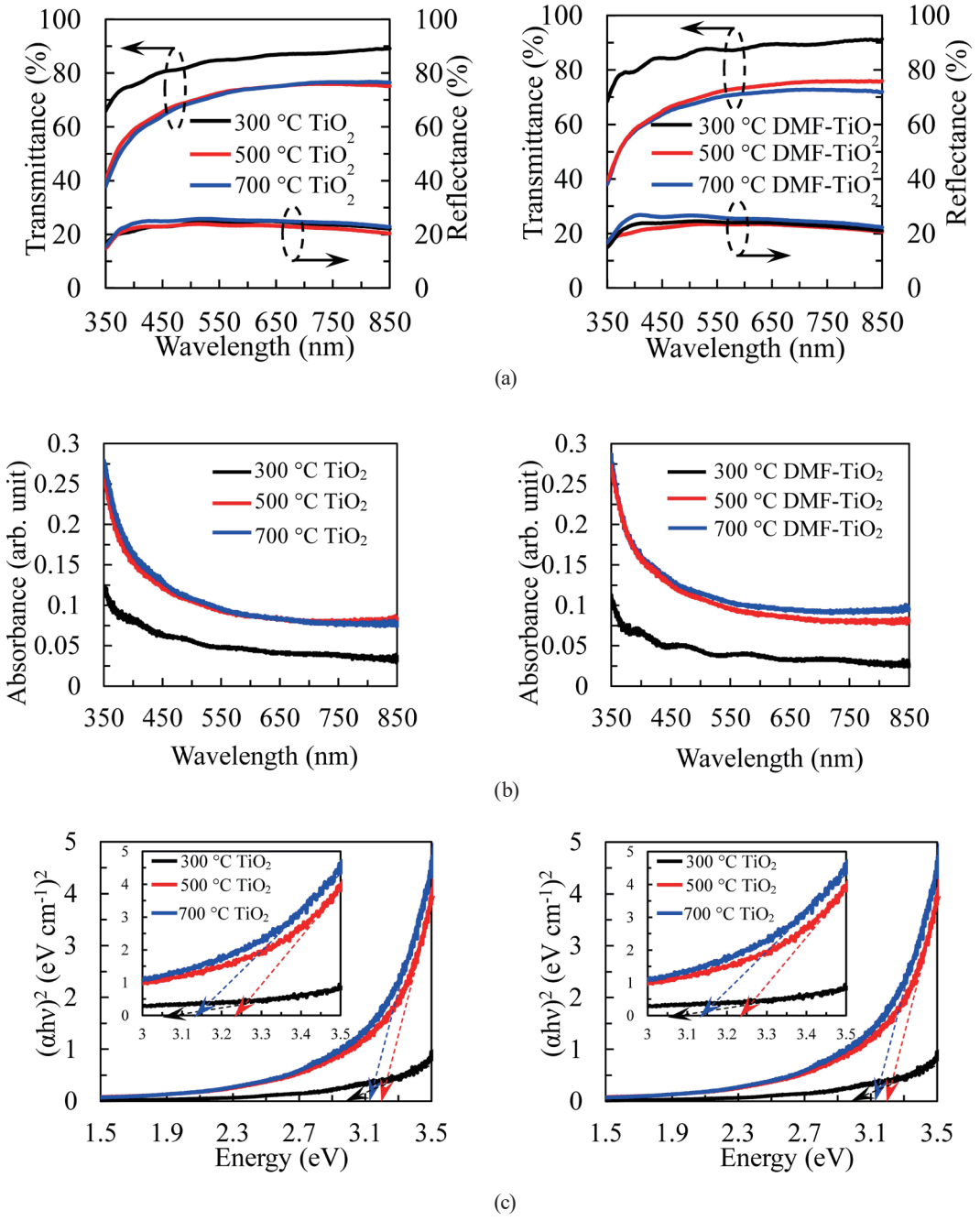

Fig. 5. (Color online) (a) Transmittance and reflectance, (b) absorption, and (c) calculated energy gap for TiO_2 films (left) and DMF-TiO_2 films (right) annealed at 300, 500, and 700 °C.

$$(\alpha h\nu) = K(h\nu - Eg), \tag{2}$$

where $h\nu$ is the excitation energy, K is an energy-independent constant, and Eg is the optical energy gap of the direct TiO_2 thin films.[27] The direct band gap (n = ½) value is obtained from the x-intercept of the extrapolated linear part of the graph of $(\alpha h\nu)^2$ versus the photon energy, as

Table 2
Average transmittance (Ave-T%) and reflectance (Ave-R%) in the 400–700 nm range as well as estimated *Eg* for TiO_2 and DMF-TiO_2 films annealed at 300, 500, and 700 °C.

Parameters	TiO_2 films			DMF-TiO_2 films		
Annealing temperature (°C)	300	500	700	300	500	700
Ave-T% (%)	86.22	74.74	74.88	89.09	77.94	74.25
Ave-R% (%)	23.3	24.93	25.16	23.39	23.99	25.26
Energy gap (eV)	3.05	3.23	3.13	3.196	3.117	3.178

widely used in the literature for TiO_2.[28] The *Eg* value estimated at annealing temperatures of 300, 500, and 700 °C as well as the average value of the optical properties in the 400–700 nm range are shown in Table 2. The amorphous TiO_2 film has the highest average transmittance (Ave-T%) of 86.2% and the lowest average reflectance (Ave-R%) of 23.3% at 300 °C. With increasing annealing temperature, Ave-T% decreases to ~74.8%, while Ave-R% does not change significantly. The same variation of Ave-T% and Ave-R% is observed for the DMF-TiO_2 films since adding DMF increases the compactness of TiO_2 films and induces an obvious redshift of the absorption edge. This result causes narrowing of the band gap, decreasing *Eg* for the DMF-TiO_2 films. The amorphous TiO_2 film shows the lowest *Eg* of 3.05 eV at 300 °C. The highest *Eg* of 3.23 eV is obtained when the annealing temperature is 500 °C, then *Eg* decreases to 3.13 eV at 700 °C owing to the obvious redshift of the absorption edge. These annealed samples have Eg values similar to that of brookite TiO_2 (~3.1–3.5 eV), while the TiO_2 film annealed at 500 °C has *Eg* similar to that of anatase TiO_2.[29] On the other hand, *Eg* of the DMF-TiO_2 film decreases from 3.196 eV at 300 °C to ~3.117 eV at 500 °C, indicating a structural change of the film.

4. Conclusions

Dynamically coated TiO_2 thin films on FTO substrates were prepared with and without DMF solvent and then annealed at temperatures of 300, 500, and 700 °C. Both TiO_2 and DMF-TiO_2 films undergo a phase transition from amorphous to polycrystalline (brookite/anatase) as a result of annealing. The metastable brookite phase of the 500 °C-annealed TiO_2 film and 300 -°C-annealed DMF-TiO_2 film is inhibited when the annealing temperature is increased to 700 and 500 °C, respectively. The annealing temperature of the anatase crystal structure was successfully lowered to 300 °C by adding a small amount (1 wt%) of DMF, which also increased the compactness of the films without increasing their surface roughness, as shown by AFM images. For the annealing temperatures of 500 and 300 °C, the maximum band gap values of the TiO_2 and DMF-TiO_2 films were 3.23 and 3.2 eV, respectively. Finally, the obvious redshift of the absorption edge and the structural change contribute to the variation of *Eg* for both TiO_2 and DMF-TiO_2 films with increasing annealing temperature, suggesting the considerable potential of developing TiO_2 films with a wide band gap by adding a small amount of DMF.

Acknowledgments

This research was funded by the National Science and Technology Council (NSTC) of Taiwan under contract number: NSTC 109-2221-E-390-008. This research was also funded by

the Natural Science Foundation of Fujian Province, grant numbers 2020J05150 and 2020J05151; and the Scientific Research Projects of Jimei University, grant number ZQ2019032. We appreciate the administrative and technical support from Ms. Hsiu-Ling Huang and the Micro & Nano Semiconductor Research Center of Jimei University.

References

1 W. C. Tian, Y. H. Ho, and C. H. Chou: IEEE Sens. J. **13** (2013) 1725. https://doi.org/10.1109/JSEN.2013.2242259
2 K. I. Jang, E. Hong, and J. H. Kim: Korean J. Chem. Eng. **29** (2012) 356. https://doi.org/10.1007/s11814-011-0291-2
3 R. H. Lee, C. Y. Huang, and C. T. Chen: J. Appl. Polym. Sci. **92** (2004) 1432. https://doi.org/10.1002/app.13688
4 D. Komaraiah, P. Madhukar, Y. Vijayakumar, and M. V. Ramana Reddy: Mater. Today: Proc. **3** (2016) 3770. https://doi.org/10.1016/j.matpr.2016.11.026
5 X. Y. Xin, T. Xu, L. Wang, and C. Y. Wang: Sci. Rep. **6** (2016) 23684. https://doi.org/10.1038/srep23684
6 M. Katayama, H. Koinuma, and Y. Matsumoto: Mater. Sci. Eng., B **148** (2008) 19. https://doi.org/10.1016/j.mseb.2007.09.050
7 M. Maimaiti, B. H. Zhao, and M. Mamat: Mater. Res. Express. **6** (2019) 086408. https://doi.org/10.1088/2053-1591/ab1853
8 S. L. Xing, L. C. Lin, and G. S. Zou: Nanotechnol. **28** (2017) 405302. https://doi.org/10.1088/1361-6528/aa8150
9 B. P. Bastakoti, Y. Sakka, K. C. W. Wu, and Y. Yamauchi: J. Nanosci. Nanotechnol. **15** (2015) 4747. https://doi.org/10.1166/jnn.2015.9694
10 X. Hu, X. Zhang, X. R. Chen, and M. Luo: Nanotechnol. **31** (2020) 135209. https://doi.org/10.1088/1361-6528/ab646f
11 E. H. Alsharaeh, T. Bora, and A. Soliman: Catalysts **7** (2017) 133. https://doi.org/10.3390/catal7050133
12 G. Kignelman, W. Thielemans: J. Mater. Sci. **56** (2021) 5975. https://doi.org/10.1007/s10853-020-05607-1
13 A. Ito, T. Sato, and T. Goto: Thin Solid Films **551** (2014) 37. https://doi.org/10.1016/j.tsf.2013.11.089
14 I. W. Feng, S. X. Jin, J. Li, J. Y. Lin, and H. X. Jiang: J. Vac. Sci. Technol. A **31** (2013) 061514. https://doi.org/10.1116/1.4823705
15 S. L. Zhu, Z. H. Yu, and L. H. Zhang: ACS Appl. Nano Mater. **4** (2021) 3940. https://doi.org/10.1021/acsanm.1c00322
16 I. A. Cordova, Q. Peng, I. L. Ferrall, A. J. Rieth, P. G. Hoertz, and J. T. Glass: Nanoscale **7** (2015) 12226. https://doi.org/10.1039/C5NR90125A
17 M. B. Tahir, K. Nadeem, M. Hafeez, and S. Firdous: Indian J. Pure Appl. Phys. **55** (2017) 6. https://doi.org/10.56042/ijpap.v55i10.12312
18 B. Christ, W. Glaubitt, and K. Berberich: Materials **15** (2022) 2752. https://doi.org/10.3390/ma15082752
19 B. Wang, S. C. Wei, and L. Guo: J. Mater. Res. Technol. **19** (2022) 2171. https://doi.org/10.1016/j.jmrt.2022.06.004
20 A. Sivkov, Y. Vympina, and A. Ivashutenko: Ceram. Int. **48** (2022) 10862. https://doi.org/10.1016/j.ceramint.2021.12.303
21 S. E. da Silva, L. T. B. Mendonça, and P. L. Guzzo: Mater. Lett. **298** (2021) 130021. https://doi.org/10.1016/j.matlet.2021.130021
22 Y. J. Huang, G. Pandraud, and P. M. Sarro: J. Vac. Sci. Technol., A **31** (2013) 01A148. https://doi.org/10.1116/1.4772664
23 M. Thakurdesai, D. Kanjilal, and V. Bhattacharyya: Appl. Surf. Sci. **258** (2012) 7855. https://doi.org/10.1016/j.apsusc.2012.04.089
24 K. Manickam, V. Muthusamy, S. Manickam, T. S. Senthil, G. Periyasamy, and S. Shanmugam: Mater. Today: Proc. **23** (2020) 68. https://doi.org/10.1016/j.matpr.2019.06.651
25 C. H. Hsu, K. T. Chen, and L. S. Liang: IEEE J. Electron Devices Soc. **9** (2021) 49. https://doi.org/10.1109/JEDS.2020.3039189
26 J. Tauc: Mater. Res. Bull. **3** (1968) 37. https://doi.org/10.1016/0025-5408(68)90023-8
27 P. Deák, B. Aradi, and T. Frauenheim: J. Phys. Chem. C **115** (2011) 3443. https://doi.org/10.1021/jp1115492
28 J. P. Wang, Z. Y. Wang, and B. B. Huang: ACS Appl. Mater. Interfaces **4** (2012) 4024. https://doi.org/10.1021/am300835p
29 D. K. Muthee and B. F. Dejene: Heliyon **7** (2021) e07269. http://doi.org/10.1016/j.heliyon.2021.e07269